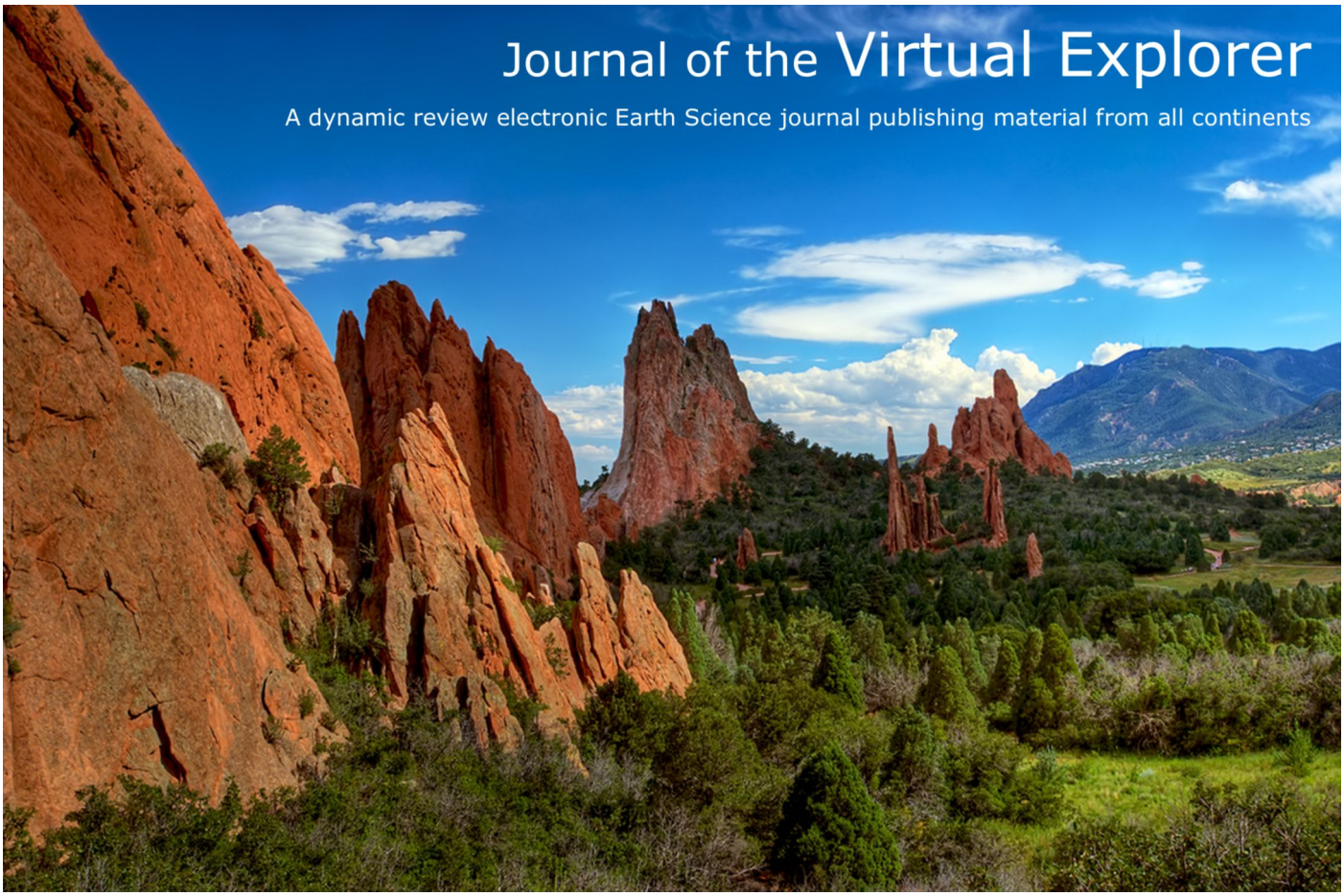

The role of fluid-inclusion composition on dynamic recrystallization in experimentally deformed quartz single crystals

Ineke Dijkstra, Joyce Schmatz, Alice Post, Janos Urai

Journal of the Virtual Explorer, Electronic Edition, ISSN 1441-8142, volume **38**, paper 3
In: (Eds.) M.A. Forster and J.D. Fitz Gerald, The Science of Microstructure - Part II, 2011.

Journal of the Virtual Explorer, 2011
Volume 38
Paper 3
http://virtualexplorer.com.au/

The role of fluid-inclusion composition on dynamic recrystallization in experimentally deformed quartz single crystals

Ineke Dijkstra
Private address

Joyce Schmatz
Structural Geology, Tectonics and Geomechanics, Geological Institute, RWTH Aachen University, Lochnerstrasse 4-20 52062 Aachen, Germany. *Email: j.schmatz@ged.rwth-aachen.de*

Alice Post
Nederlandse Aardolie Maatschappij BV (NAM), Schepersmaat 2, 9405 TA Assen, The Netherlands.

Janos Urai
Structural Geology, Tectonics and Geomechanics, Geological Institute, RWTH Aachen University, Lochnerstrasse 4-20 52062 Aachen, Germany. *Email: j.urai@ged.rwth-aachen.de*

Abstract: In order to study the effect of fluid composition on rheology and recrystallization we have deformed and annealed single crystals of natural quartz with different fluid inclusion compositions. Two samples contained mainly aqueous inclusions; one sample contained more gaseous inclusions. The samples were deformed in a Griggs-type solid medium apparatus at 1200 MPa confining pressure, temperatures ranging from 710 to 820°C and strain rates between 0.9 x 10^{-6} s^{-1} and 11 x 10^{-6} s^{-1}. After deformation samples were held between 800-900°C and annealed for 2-279 hours. The gas-rich samples have a significantly higher strength than samples containing aqueous inclusions, resembling dry quartz samples. We relate the difference in strength to an effect of fluid composition on dislocation climb and/or glide.

Quartz recrystallized in all samples but recrystallization is much slower in the gas-rich samples. Recrystallized grains are elongated perpendicular to the shortening direction. They contain many fewer fluid inclusions than the starting material and many inclusions are found in their grain boundaries. This suggests that the fluid segregates to the grain boundaries during migration. The elongated shape may result from differences in thickness of a fluid film on the grain boundaries parallel and perpendicular to the shortening direction.

Citation: 2011. The role of fluid-inclusion composition on dynamic recrystallization in experimentally deformed quartz single crystals. In: (Eds.) M.A. Forster and J.D. Fitz Gerald, *Journal of the Virtual Explorer*, volume **38**, paper 3, doi: 10.3809/jvirtex.2011.00281

Introduction

The interaction of fluid and rock during deformation plays an important role in numerous processes inside the Earth's crust. The presence and composition of fluids affects rock properties, such as rheology and transport, on different scales and by a variety of processes. Understanding these processes is needed for extrapolation of rheology or paleo-conditions from experiments to nature, and to determine the reliability of, for example, temperature and paleostress estimates. This effect is important for free fluid as well as for fluid occurring in inclusions.

Since quartz is an important component of the Earth's continental crust and fluids are thought to occur abundantly at depth, it is important to understand the interaction of the fluid with the quartzite. It is well known that water affects the deformation of quartzites in nature and in experiments (e.g., Jaoul *et al.*, 1984; Kronenberg *et al.*, 1990; Post and Tullis, 1998), though the process of weakening is not yet understood in detail and there is still much debate about the exact role of fluids in deformation mechanisms (e.g., den Brok, 1992, Wang, 1992, Rutter and Brodie, 2004; Stipp *et al.*, 2006). Early experimental work on understanding quartz deformation in the presence of fluids has been performed with pure water (e.g, Jaoul, 1984 and references therein). However, the fluids that occur in the crust are not pure H_2O, and FTIR studies on natural quartz suggest more CO_2-rich fluids at depth (e.g., Nakashima *et al.*, 1995). Some work has been done on effects of the fluid composition (Post *et al.*, 1996; Wang *et al.*, 1993; Wang, 1992; Ord and Hobbs, 1986) and a recent study by Chernak *et al.* (2009) shows the effect of aqueous and carbonic fluids on the strength of quartz taking into account the chemical environment, such as the effect of reducing and oxidizing conditions. Post *et al.* (1996) varied the water fugacity in experiments on Heavitree quartzite by changing the confining pressure and found evidence that water fugacity affected the dislocation creep strength. They studied the effect of varying fluid composition (pure water or 90% CO_2) on the rate of dislocation climb and recrystallization and observed higher rates of dislocation climb and recrystallization in the samples with pure water added.

Recrystallization is almost always strongly affected by the presence of a second phase. The effect depends on the type of second phase and several other parameters. The presence of a solid second phase will in general decrease the average grain boundary mobility, i.e., it will pin the grain boundary or drag may occur (Olgaard and Evans, 1988; Herwegh and Berger, 2004, Schmatz and Urai, 2010; Schmatz *et al.*, 2011). When the driving force is high enough the boundary may break free of the particles (Drury and Urai, 1990). The interaction with a fluid phase is somewhat different and depends on the type of fluid. When the fluid is a solvent for the mineral, its presence may increase the grain boundary mobility because it enhances the across-boundary diffusion rate, e.g., in 1968 Hobbs showed that dry samples of quartz did not recrystallize under conditions where water-wet samples did (see also Tullis and Yund, 1982). A similar role of water was found for static grain growth in anorthite (Dresen *et al.*, 1996). However, if the mineral is not soluble in the fluid phase the second phase will not increase the migration rate but may even pin the grain boundaries (e.g., calcite at high temperature, Tullis and Yund, 1982, or air: Olgaard and Evans, 1988). Schmatz and Urai (2011) show that oxidant bearing grain boundaries in quartz have the ability to transform solid graphite into CO_2 in a naturally deformed and partly recrystallized quartz vein from the Hunsrück slate, Germany. They also show that various interactions of grain boundaries, moving at different velocities, with fluid inclusions are responsible for significant redistribution and modification of the fluid phase at different rates.

Fluid-enhanced recrystallization has also been attributed to the wetting characteristics of the fluid with the solid, i.e., if the fluid wets the solid the grain boundary migration rate would increase as more surface was exposed to a fast diffusion environment. It is therefore useful to consider what "wetting" means. Under equilibrium conditions a fluid will only fully wet a grain boundary (wetting angle = 0°) if the surface energy of the solid-liquid interface is equal to or smaller than half that of the solid-solid interface ($\gamma_{ss}/\gamma_{fs} = 2 \cos (a/2)$, where $\gamma_{ss}$is the solid-solid interfacial energy, γ_{fs} is the liquid-solid interface energy, and α the dihedral, or wetting angle; e.g., Watson *et al.*, 1990; Laporte, 1994, Holness, 1992; 1993). However, a moving grain boundary or a boundary under load is not in thermodynamic equilibrium and thus the properties of the boundary may be different from that in equilibrium, and a continuous fluid film may exist on such a boundaries. This phenomenon has been suggested from several experimental studies (e.g., Urai, 1983; Urai *et al.*, 1986; Jin *et al.* 1994; Drury and Fitz Gerald, 1996; Tullis *et al.*, 1996; Bai *et al.*, 1997; Rutter and Brodie,

2004; Schenk and Urai, 2005, Schmatz and Urai, 2010; Schmatz *et al.*, 2011). When using the term wetting in this paper we refer to this non-equilibrium situation, not the thermodynamic equilibrium case.

The interaction between grain boundaries and fluid inclusions during recrystallization is dependent on the fluid composition. This is important since fluid inclusions give information about paleo-temperature in the rocks. Holness (1995) points to the effect of fluid-composition on wettability, which is a major parameter controlling the pore fluid distribution. Drury and Urai (1990) have proposed that H_2O -rich fluids form continuous fluid films on moving grain boundaries, whereas CO_2-rich fluids do not, based on observations in natural rocks. They suggested that a moving grain boundary may significantly change the fluid inclusion composition when CO_2 is preferentially partitioned to inclusions, and H_2O remains on the boundary. A release of H_2O can be even promoted taking into account moderately reducing conditions (Chernak *et al.*, 2009). Thus errors can occur when using fluid inclusions for paleo-thermometry. These issues were already addressed in studies dealing with the effect of decrepitation on the composition of fluid inclusions (e.g. Bodnar *et al.*, 1989; Sterner and Bodnar, 1989), also with respect to the role of (pipe) diffusion (Bakker and Jansen 1991,1994; Hall and Sterner, 1993) and the effect of hydrogen diffusion through the quartz lattice (Mavrogenes and Bodnar; 1994; Morgan *et al.*, 1993; Rutter and Brodie, 2004). There are several studies that discuss the effect of deformation on H_2O-loss from fluid inclusions (e.g., Kerrich, 1976; Hollister, 1990; Johnson and Hollister, 1995; Audétat and Günther, 1999; Vityk *et al.*, 2000; Tarantola *et al.*, 2010) but the role of grain boundary migration (Drury and Urai, 1990; Schmatz and Urai, 2011) is not often considered. Grain boundary diffusion can be a much faster process than lattice diffusion (Atkinson, 1984), and is accordingly important to understand. However, the effect of grain boundary migration on the composition of fluid inclusions has not been given much attention.

With this study we present some preliminary results that show an effect of the ratio of aqueous and gaseous inclusions on rheology and recrystallization. We have deformed single crystals of quartz that contain fluid inclusions with different aqueous-gaseous inclusion ratios and observed strength and microstructure as a function of fluid composition. The samples recrystallized during deformation and during a post-kinematic annealing period and the effect of recrystallization on the distribution and composition of fluid inclusions was studied. We believe these results are important and representative for processes of wide relevance but more experiments and systematic observations are needed to fully understand the process.

N.B. This paper based on the results of the master thesis by I. Dijkstra (1990). All results are presented here as described coherent with that study. We were not able to include further analytics, as the samples were not available anymore.

Experimental methods

Starting materials

Three types of quartz single crystals with different fluid inclusions compositions were used in this study, originating from Victoria (Australia), Naxos (Greece, Schuiling and Kreulen, 1979), and Scandinavia (Table 1).

The fluid inclusions that occur in these samples can roughly be divided into three categories: large, medium, and small inclusions. Detailed descriptions of the quartz and the inclusions are given below. The fluid composition in our starting materials was determined using a heating stage in optical microscopy. We did not characterise the water related point-defect structure of the samples by FTIR (Keppler and Rauch, 2000). The large quantity of bulk water in fluid inclusions makes FTIR characterisation of point defects very difficult. Therefore we cannot determine a possible interaction between properties of the samples and their point defect structure, but only with the bulk fluid composition.

The Victoria samples are milky vein quartz with straight extinction, with approximately 4 vol.% fluid inclusions. The larger fluid inclusions occurring in clusters are 20-40 μm in size and irregular in shape. These inclusions contain 0-20 vol.% gas and 80-100 vol.% liquid. The medium size inclusions (5-10 μm) are homogeneously distributed throughout the grains and have a smooth shape. They contain 0-20 vol.% gas and 50-100 vol.% liquid, and 0-30 vol.% solid (in the form of cubic crystals). The small inclusions are found in trails and have a spherical shape. These inclusions are 1-5 μm in size and contain 0-70 vol.% gas and 30-100 vol.% liquid (Table 2).

Table 1. Experimental conditions and details.

Experiment #	**25**	**27**	**30**	**32**	**33**	**34**
Starting material	Victoria	Victoria	Victoria	Naxos	Scandina-via	Naxos
Fluid inclusions (main phase)	aqueous	aqueous	aqueous	gaseous	aqueous	gaseous
c-axis*	76	76	56	81	86	84
T (deformation)	810	710	780	810	820	815
strain rate ($x10^{-6}/s^{-1}$)	0.9	10	11	9	11	3.8
P confining (GPa)	1.16	1.17	1.16	1.17	1.16	1.16
T (deformation)	810	710	780	810	820	815
σ_1-σ_3 (MPa)	320	590	450	1240	640	1500
T (annealing under stress)	800	800	900	820	820	820
t (annealing under stress) h:m	2:20	107:30	32:30	97:30	279:05	78:20
Recrystallized area (%)	1	30	15	10	30	10
Capsule	Au	Au	Pt	Pt	Pt	Pt

**Cylindrical samples (length ~12 mm, diameter 5.9 mm) were cored at an angle of 56 – 86° with respect to the c-axis.*

The material from Naxos has faint undulose extinction and contains ~1-2 vol.% fluid inclusions which are inhomogeneously distributed in clusters and along healed cracks. The large, 5-20 μm fluid inclusions contain 20-100 vol.% gas and 0-80 vol.% liquid. These inclusions are irregular and prolate in shape. Small inclusions (<5 μm) contain only gas (Table 2).

The quartz from Scandinavia is clear to milky, contains 4-5 vol.% fluid inclusions, and has blocky undulose extinction. Large inclusions (10-35 μm) are irregular in shape and cluster along healed cracks. These inclusions contain 0-60 vol.% gas, but mostly in the range of 10 vol. %. Medium-size inclusions are 1-5 μm in size and spherical to round in shape. They contain 10 vol.% gas and 90 vol.% liquid, and infrequently they also contain cubic crystals, inferred to be NaCl. The small, spherical inclusions of 0.5-3 μm contain liquid.

Sample assembly

Cylindrical samples (length ~12 mm, diameter 5.9 mm) were cored at an angle of 56° - 86° with respect to the c-axis (see Table 1). Samples were bench-dried and then weld-sealed in thick-walled gold or platinum capsules (Table 1). The samples were deformed in a Tullis-modified Griggs-rig (Tullis and Tullis, 1986) at the Utrecht University, The Netherlands, using an all-salt assembly (for details see den Brok, 1992). For this type of assembly no pressure correction is required (Johannes, 1978).

Experimental procedure

Stresses were applied at temperatures between 710 and 820°C, 1200 MPa confining pressure and strain rates ranging from 0.9 to 11 x 10^{-6} s^{-1} (see Table 1). In order to avoid decrepitation of the fluid inclusions as much as possible during heating and pressurisation of the samples, the pressure and temperature were raised along the isochore of water density (1 gcm^{-3}, Fisher, 1976). Samples were then axially shortened to bulk strains ranging from 6.5 - 38.4 %. After the deformation the samples were held at high temperature and pressure for various time periods (2 – 280 h) allowing annealing and static recrystallization of the samples. Annealing temperatures were similar to or higher than temperatures during deformation (Table 1). At the conclusion of deformation, the σ_1–piston was not reversed, so that the samples annealed under stress. At the conclusion of each experiment the sample was cooled rapidly in order to avoid changes in microstructure. We prepared standard thin-sections (30 μm) parallel to the shortening direction. Stress-strain curves

were calculated from the force-displacement record assuming homogeneous shortening of the sample and assuming the same linear increase in friction before and after the top piston reaches the sample (den Brok, 1992).

Slabs of material 1 mm thick were cut parallel to the shortening direction and prepared for Scanning Electron microscopy (SEM, glued to SEM stubs and carbon and gold coated). The slabs were carefully broken along planes either parallel to σ_1 or perpendicular to σ_1. The polycrystals break along the grain boundaries of recrystallized grains and this method thus allows observation of the grain boundary morphology (see also Urai 1983, Olgaard and Fitz Gerald, 1993; Mancktelow *et al.* , 1998).

Table 2. Fluid inclusion types and distribution.

Material	**General**	**Large**	**Medium**	**Small**	**Exp #**
Fluid inclusion characteristics in starting material					
Victoria	Grains with straight extinction and 4 vol.% fluid inclusions.	20-40 μm in diameter, with 0-20% gaseous and 80-100% aqueous inclusions, irregular in shape and arranged in clusters.	5-10 μm in diameter, with 0-20% gaseous, 50-100% aqueous and 0-30% solid, cubic inclusions. All are smooth in shape. The distribution is homogeneous.	1-5 μm in diameter, with 0-70% gaseous, 30-100% aqueous inclusions occurring in trails infrequently containing salt. The shape is spherical.	25
Scandinavia	Blocky grains with undulose extinction and 4-5 vol.% fluid inclusions.	10-35 μm in diameter, with 0-60 % (mostly 10%) gaseous inclusions. They are irregular in shape and cluster along cracks.	1-5 μm in diameter, with 10% gaseous, 90% aqueous inclusions, infrequently containing salt. The shape is spherical.	Aqueous inclusions with 0.5-3 μm in diameter. The shape is spherical.	33
Naxos	Grains with faint undulose extinction and 1-2 vol.% fluid inclusions, in-homogeneously distributed.	5-20 μm in diameter, with 20-100% gaseous and 0-80% aqueous inclusions. They are irregular and prolate in shape and some appear along healed cracks.	-	Only gaseous inclusions smaller than 5 μm in diameter.	32 + 34
Fluid inclusion characteristics after deformation					
Victoria	Small and large inclusions are found along grain boundaries. In non-recrystallized areas the fluid inclusion distribution has not changed.	5-20 μm in diameter with irregular shape, some snaffle-shapes, often elongated parallel to σ_1.	0.3-3 μm in diameter, split up into larger number, often with round shapes.	Usually arranged in trails.	25

Material	General	Large	Medium	Small	Exp #
Victoria	Fluid inclusions in bands, 50-150 μm long and sub-parallel to σ_1 arranged in clusters. Recrystallized grains are free of fluid inclusions. Many elongated inclusions along grain boundaries with extra large ones on triple junctions, sometimes connected by fluid films.	2-15 μm in diameter with 20-30% gaseous inclusions.	Smaller than 2μm.	Appear in trail at 70° relative to σ_1.	27
Victoria	Fluid inclusions are homogeneously distributed outside recrystallized areas and cluster on grain boundaries. Recrystallized grains contain no inclusions, except some large gaseous ones, also along grain boundaries.	5-40 μm in diameter with very irregular shape.	Smaller than 3 μm in diameter, with no changes in shape.	No planar arrays.	30
Scandinavia	Recrystallized grains contain only few fluid inclusions (< 0.5 μm), also along grain boundaries. Large inclusions are found in "pressure shadows" of recrystallized grains. In non-recrystallized areas fluid inclusions are homogeneously distributed. In recrystallized areas inclusions cluster on triple junctions (SEM). Some large inclusions on triple junctions are connected by fluid films.	Around 20 μm in diameter.	Elongated perpendicular to σ_1, around 3-8 μm long and 1-2 μm wide.		33
Naxos	Fluid inclusions are small (<4 μm) and arranged in bands. Large, elongated inclusions on grain boundaries, less inside recrystallized grains. Small inclusions appear also in recrystallized grains, but less than in non-recrystallized.				32 + 34

Results

Mechanical data

The samples from Naxos with gaseous fluid inclusions have a much higher strength than those with aqueous inclusions. The two samples with gaseous inclusions (experiments 32 and 34) reached a differential stress of ~1300 MPa, but did not reach a steady state flow stress (Fig. 1). The samples with aqueous inclusions, deformed with flow stresses of 320 (10^{-5} s^{-1}) and 450-650 MPa (10^{-5} s^{-1}; both Victoria and Scandinavia samples, experiments 25, 27, 30, and 33; Fig. 1). There is scatter in sample strength for different starting materials as well as for the same material. This variability in strengths may be related to the c-axis orientation in the sample, and to

inhomogeneous distribution of fluid inclusions. However, the difference in strength between samples with different fluid inclusions composition is too large to be due to one of these factors and we therefore interpret it related to fluid composition.

Figure 1. Stress-strain curves of the deformation experiments

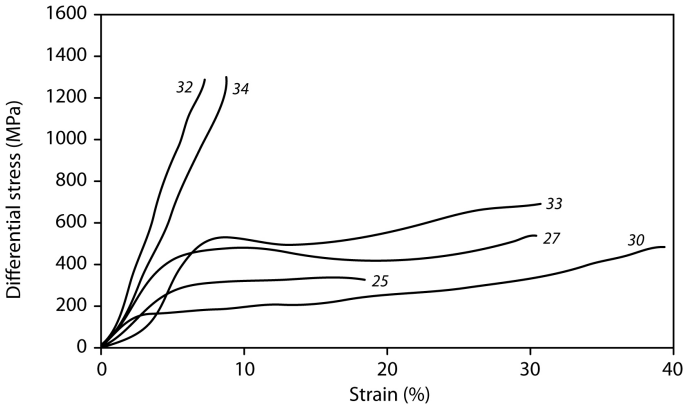

Curves labelled 32 and 34 refer to gas-rich Naxos quartz, 25, 27 and 30 to Victoria samples, and 33 to Scandinavia material, both rich in aqueous inclusions. Details on the experiments are listed in Table 1.

Microstructures

All samples with aqueous inclusions have similar microstructures after deformation and annealing. They contain recrystallized grains showing straight extinction, which is in contrast to the original material showing undulose extinction (Fig. 2a and c). The sample that was annealed for 2 hours (experiment 25, Table 1) has 1 vol. % recrystallized grains; the samples that were annealed for longer times have more recrystallized grains, indicating that most recrystallization occurred during the annealing stage of the experiment. Recrystallized grains are elongated perpendicular to the shortening direction and their size varies somewhat with annealing/recrystallization time, but reaches > 100 μm in all samples. The recrystallized grains are normally free of internal fluid inclusions (Fig. 2b and f), but occasionally contain some large, gaseous ones. However, in some cases many fluid inclusions exist along boundaries of the recrystallized grains (Fig. 2f).

Samples with gaseous inclusions have different microstructures compared with those containing aqueous inclusions. Recrystallized grains also are elongated perpendicular to the shortening direction, but the grains are smaller in size. In these samples fluid inclusions are found inside the recrystallized grains, though somewhat less than in the surrounding quartz, and also on grain boundaries.

Several different features are observed in SEM on the grain boundaries in the H_2O-rich samples (Figs. 3a-c): Grain boundaries in between unrecrystallized grains are irregular with many pits of fluid inclusions (Fig. 3a). In contrast, the grain boundaries of the recrystallized grains are often smooth or exhibit channel-like features (Fig. 3b and c). Grain boundaries of recrystallized grains have rough interfaces in some cases, but are less distinct than the unrecrystallized areas (Fig. 3d-f). Triple junctions are often open (Fig. 3d-f). On the edges of the triple junction channels irregular channels are found in some cases (Fig. 3f).

Figure 2. Optical micrographs

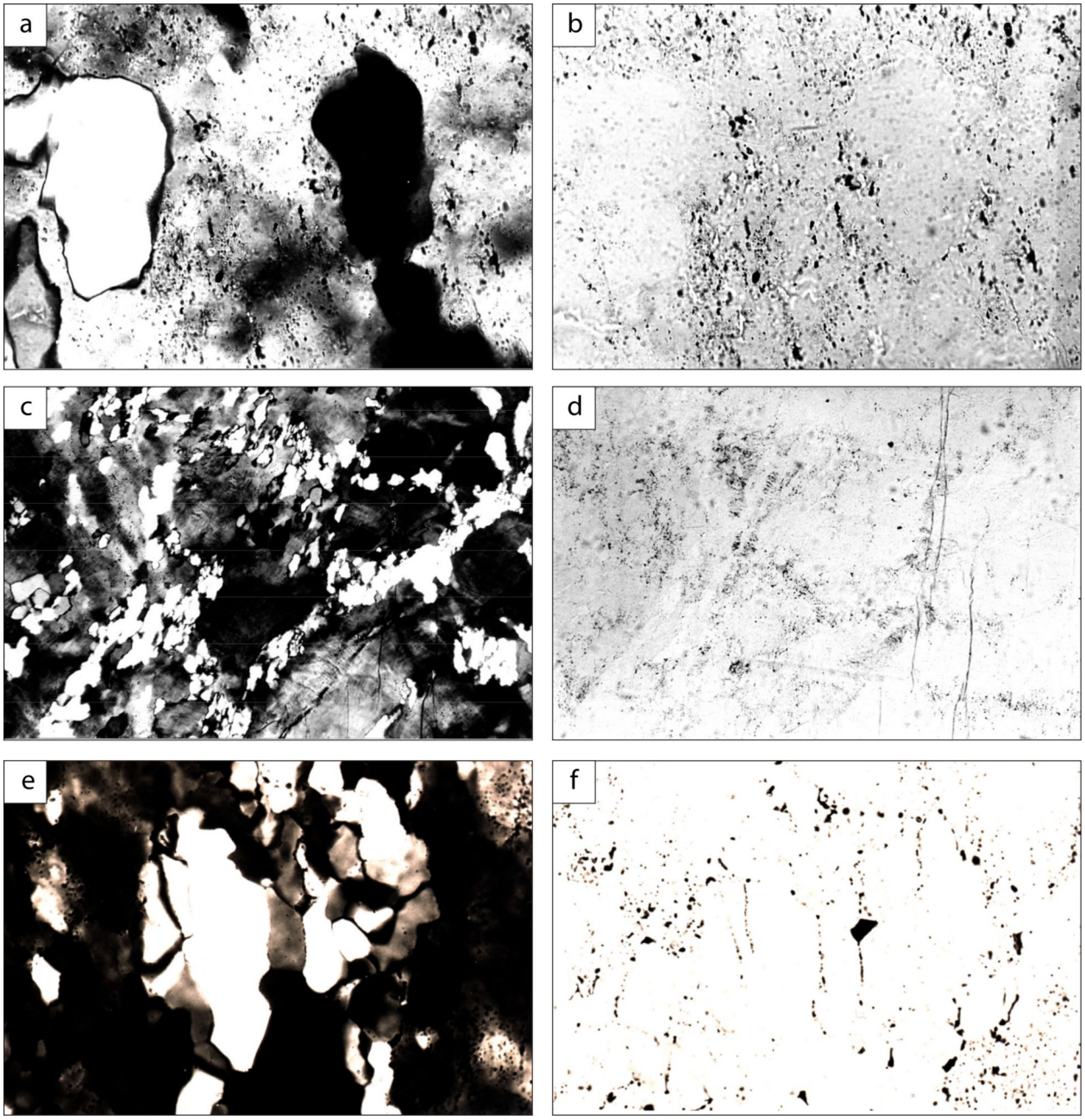

Images a,c, and e had crossed polarisers while b,d, and e had plane polarised illumination.

a and b) Sample 27, illustrating elongated recrystallized grains with straight extinction and udulatory extinction in surrounding material. Fluid inclusions are concentrated on grain boundaries. Shortening direction is horizontal (width of photos is 140 µm).

c and d) Sample32, overview of recrystallized grains in matrix with undulatory extinction. Shortening direction is horizontal (width of photos is 5.5 mm).

e and f) Sample 33, recrystallized grains contain fewer fluid inclusions as the original material, there are fewer inclusions on grain boundary than in sample 27 (a-b). Shortening direction is horizontal (width of photos is 140 µm).

Figure 3. Scanning electron micrographs of sample 33

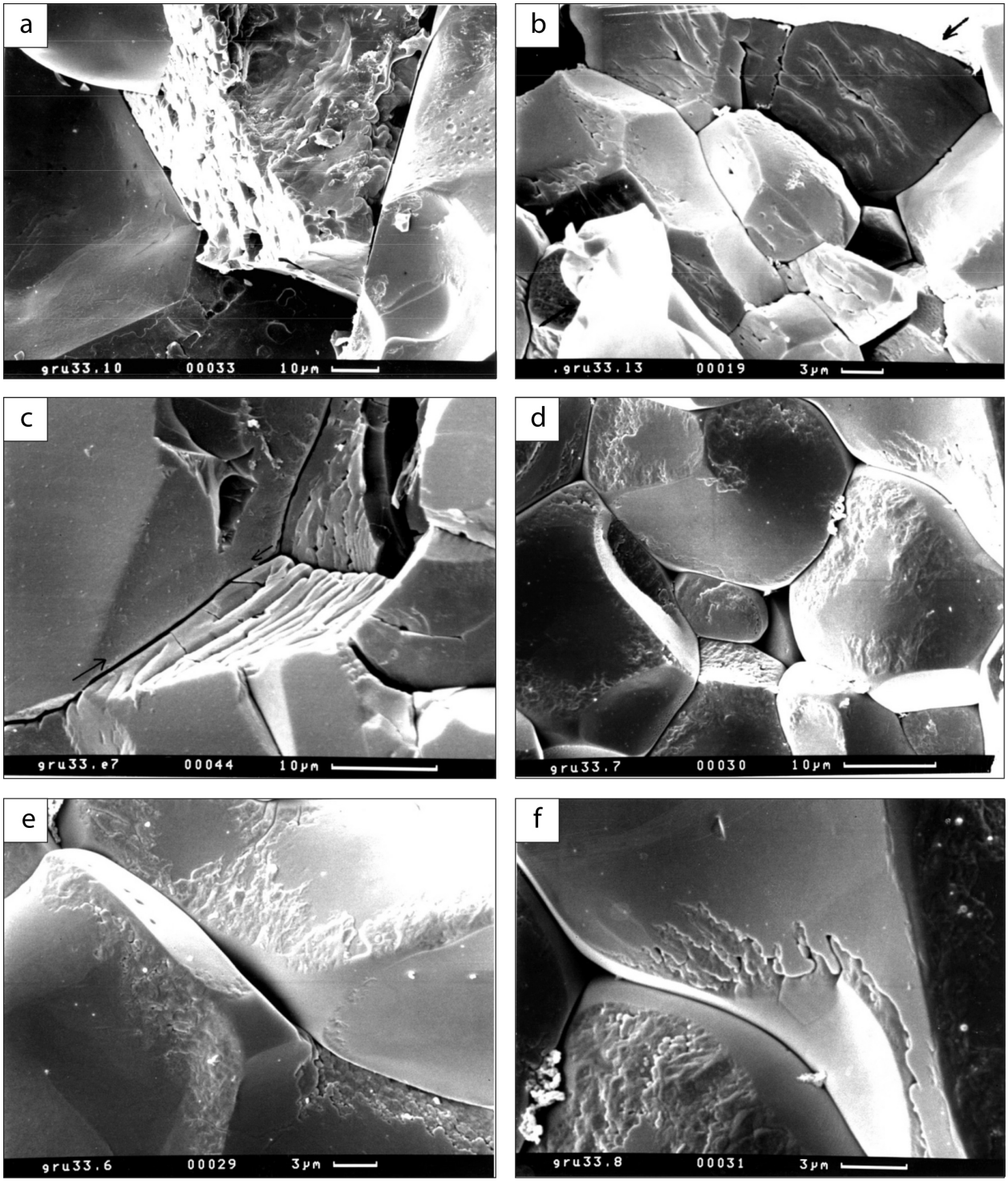

The polycrystals break along grain boundaries:
a) Starting material containing many fluid inclusions in the center and inclusion-free recrystallized grains surrounding it;
b) Recrystallized grains showing channel-shaped features on their grain boundaries;
c) View is similar to b) but lower magnification;
d) Smooth grain boundaries and open triple junctions;
e) Lens-shaped pores on grain boundaries;
f) Open triple junctions and irregular features possibly representing healing of the boundary.

Fluid inclusions

The size and distribution of fluid inclusions changed during the experiments as listed in Table 2 and described below:

The sample of Victoria quartz annealed under stress for 2 hours after deformation (experiment 25). It has large and small fluid inclusions along grain boundaries of recrystallized grains. In non-recrystallized regions the distribution of inclusions has not changed. In general, fluid inclusions decreased in size (see Table 2), and increased in number, suggesting the original inclusions have split up and re-annealed. In some cases this process is illustrated by elongated inclusions that narrow down towards the centre (Fig. 2f). Inclusions are often elongated parallel to σ_1. The sample that was annealed for 32 hours at 900°C (experiment 30) has ~15% recrystallized grains and the distribution of fluid inclusions has not changed in the unrecrystallized areas. In the regions with recrystallized grains the fluid inclusions occur preferentially along grain boundaries and have decreased in size compared to the starting material. In the sample with the most recrystallized grains (30%) that was annealed the longest (experiment 27, 107 h at 800 °C) fluid inclusions appear in clusters and bands sub-parallel to σ_1. Inclusions occur on grain boundaries of recrystallized grains and are elongated. Outspread depressions along grain surfaces are interpreted representing fluid films which connect the inclusions (Fig. 3f).

At conclusion of the experiment the Scandinavia quartz sample, experiment 33, has approximately 30% recrystallized grains, similar to experiment 27, and shows some other features similar to that sample. Fluid inclusions that occur on the grain boundaries of recrystallized grains are large and in some cases connected by fluid films. This feature is also inferred based on the SEM observations on this sample (Fig. 3). In this sample the fluid inclusions have also decreased in size and increased in number. The recrystallized grains contain very few inclusions. The large inclusions are concentrated in the pressure shadow regions of the recrystallized grains.

In the gas-rich Naxos samples, experiments 32 and 34, there are around 10% recrystallized grains. Large, elongated fluid inclusions are found along grain boundaries of recrystallized grains, and some inside the grains. Small inclusions occur in recrystallized and unrecrystallized regions (more in unrecrystallized), and are aligned in bands.

Discussion

The samples with abundant gaseous fluid inclusions had very high strengths and did not reach a steady state flow stress, indicating that recovery was inhibited in these samples (Fig. 1, Selverstone, 2005). Samples with aqueous inclusions had a lower strength under similar conditions. This difference suggests that samples containing gas-rich inclusions behave similar to dry samples, i.e., with a lower recovery rate. This is consistent with the experiments of Post *et al.* (1996). They showed that dislocation climb and recrystallization is dependent on water fugacity. However, they only showed this dependence in pure annealing experiments and did not directly relate the nature of the fluid to strength. Our experiments do show this direct relationship. Though we cannot quantify the water-fugacity in our samples, this paper is presenting a detailed study on the effect of different kinds of fluid composition on the deformation behaviour of natural quartz with different starting fluid inclusion populations, and allows interpretation of the processes that are affected.

Dislocation creep involves several processes. Dislocations can be generated at micro-scale fluid inclusions (impurity) (McLaren *et al.*, 1989; Vityk *et al.*, 2000) and in natural samples these sources are usually abundant. At conclusion of the experiments all samples show undulose extinction indicating the presence of dislocations (Fig. 2). This suggests that the fluid composition has minor effect on the formation of dislocations.

The second process that occurs during dislocation creep is gliding of dislocations. Our experiments do not show whether fluid composition affects this process. Since deformation is accompanied by recovery processes with rate controlling grain boundary bulging and dislocation climb (compare Hirth and Tullis, 1992) we cannot distinguish an effect of fluid composition on dislocation glide.

The nature of the fluid likely has an effect on both, the dislocation climb rate and the grain boundary migration rate. Since the samples are single crystals there are initially no grain boundaries. Thus, at low strains grain boundary migration cannot contribute to the low strength, so climb is interpreted to be involved. Grain boundary migration can only operate after subgrains are rotated enough to form high angle grain boundaries, or after nucleation of new grains along grain boundaries (Hippert

and Egydio-Silva, 1996), or after early stage micro-cracking followed by healing and the formation of nuclei (Tarantola *et al.*, 2000). The samples with gaseous inclusions are stronger than those with aqueous inclusions right from the start. So the fluid composition is interpreted to affect the climb rates of dislocations at this stage, consistent with the data from Post *et al.* (1996).

Recrystallized grains

The difference in size and number of recrystallized grains between samples containing gaseous and those containing aqueous inclusions (Fig. 2) indicates that grain boundary migration is enhanced by the aqueous phase relative to the gaseous phase. Since the gas-rich samples had a much higher strength it can be assumed that they built up a much higher dislocation density than samples with aqueous fluid inclusions. Higher differences in dislocation densities should enhance the grain boundary mobility, however grain boundary mobility appears much lower or retarded in the presence of the gas inclusions. The fluid is thought to affect the grain boundary mobility in two different ways, related to the assumption that the gaseous phase is CO_2-rich and the aqueous phase is water-rich. First the quartz is less soluble in the CO_2, thus the flux of quartz across the grain boundary will be lower and the mobility of the grain boundary arguably also lower in the CO_2-rich case. The second effect is due to "wetting" of the grain boundaries. H_2O -rich fluid will form films along grain boundaries which enhance the grain boundary mobility (Urai, 1986; Rutter and Brodie, 2004). CO_2-rich fluids do not form such films but remain in isolated inclusions and may even inhibit migration by acting as a pinning second phase (Herwegh and Berger, 2004). However, as there is no comparison to dry samples provided in this study, the effect of H_2O on the flow strength cannot be estimated. The study by Stipp *et al.* (2006) suggests a negligible effect of H_2O on the recrystallized grain size of quartz and, by inference, on grain boundary mobility.

An H_2O-CO_2 effect was suggested by e.g., Drury and Urai (1990) who proposed that a H_2O-rich phase wets the grain boundary during migration, whereas a CO_2 -rich fluid does not. We have not observed the boundaries during migration, but some indication of the fluid geometry is given by the SEM observations on the broken surfaces of the samples (e.g., experiment 33, Fig. 3). Samples containing aqueous fluid inclusions are characterized by smooth grain boundary surfaces, whereas the grain boundaries in gas-rich samples are more irregular. This difference in geometry suggests an aqueous fluid film but isolated gas inclusions. Samples with aqueous fluid inclusions have open triple junctions, whereas the gas-rich samples do not. We also see this in areas where grain boundary migration stopped and the boundaries show evidence for static recrystallization (i.e., straight grain boundaries, 120° junctions). Here the fluid has pulled back into isolated inclusions. This difference in fluid distribution dependent on the composition in the statically recrystallized areas of the sample is consistent with the observations of Holness (1993). She showed that at experimental conditions similar to ours the wetting angle of H_2O in quartz was < 60°, but that CO_2-fluid has a wetting angle of > 60°.

A striking observation is that the recrystallized grains were elongated in the direction perpendicular to σ_1. Mostly the elongation of the grains was stronger than that of the total strain ellipse, which indicates that the grains also grew after the bulk shortening perpendicular to the maximum applied stress. There are several factors that may explain this effect. A likely cause is an effect of orientation dependent grain boundary mobility, due to fluid film thickness. As hypothesized by Urai *et al.* (1986), the migration rate of a grain boundary is dependent on the thickness of the fluid film, which is affected by the film orientation relative to the principal stresses. Drury and Urai (1990) suggested that the fluid film thickness is a function of boundary orientation with respect to stress direction, with thicker films on boundaries parallel to σ_1. If our recrystallizing grains showed increasing migration rate with film thickness, a faster migration rate would be expected perpendicular to σ_1. For very thin films, the migration rate will increase with film thickness till a certain limit, after which increasing film thickness will result in a decreasing migration rate, due to an increase in diffusion path length. Similar results were found by Karato and Masuda (1989) for grain growth in deformation experiments at high stresses.

A second possible cause for the elongated grains is grain growth similar to an anti-crack mechanism. The small, recrystallized grains are dislocation free and thus weaker than the strain-hardened surroundings. During stress relaxation they will deform more easily and cause stress concentrations in the surrounding material at those edges which are parallel to σ_1. The strain energy

gradients in those regions then increases, leading to an increase in the driving force for migration and thus faster migration in the direction perpendicular to σ_1. However, since the elongation of recrystallized grains is observed in all samples it is unlikely that growth anisotropy is solely responsible for the elongation. In the gas-rich samples the stress remaining after deformation is very high, and thus a slight increase in dislocation density is unlikely to cause very large differences in driving force.

Changes in fluid inclusions

During the experiment the fluid inclusions increase in number and decrease in size, suggesting that they break up during the experiment. We observe this modification in all samples, even the one that has been annealed for a very short time. We also see this phenomenon in most areas of the sample, whether recrystallization occurred or not. These observations suggest that the breaking up of fluid inclusions is not related to the recrystallization, but happens during loading and deformation of the sample by intracrystalline leakage along mobile dislocations (Kerrich, 1976, Hollister, 1990; Vityk *et al.*, 2000; Tarantola et al., 2010; Schmatz and Urai, 2011). Fluid inclusions may develop an internal overpressure and form microcracks (Roedder, 1984; Tullis and Tullis, 1985) that subsequently heal into trails of smaller inclusions (e.g., Fitz Gerald *et al.*, 1991).

Recrystallization causes some important changes in the fluid volume as the recrystallized grains contain very little fluid inclusions, whereas the starting material contained approximately 4 vol.% fluid. This raises the question where the fluid has gone. Even if the recrystallized material contains no optically visible fluid inclusions, some fluid may have been incorporated into the crystal structure as point defects (max. ~40ppm, Paterson, 1986; 1989), or point defect clusters with sub-microscopic scale fluid inclusions similar to the type that have been observed in milky quartz or amethyst respectively (Kekulawala *et al.*, 1978; Aines and Rossman, 1984). Milky quartz may contain up to 2000 H/10^6 Si; amethyst contains up to 3000 H/10^6 Si, which corresponds to ~1 vol% water. There thus remains ~3 vol% water unaccounted for that must have been swept by the boundary. This fluid must have interacted with the grain boundary in some way, since the inclusions clearly did not remain in the same position after the boundary has swept by. Thus there must be a lateral fluid pathway on the grain boundary which allows transport of fluid which has been proposed in many studies dealing with the water fugacity of quartz (e.g., Stipp *et al.*, 2006). We may see some evidence for this in the SEM, on the surfaces of samples broken along the grain boundaries (Fig. 3). The open boundaries may heal when the grain boundary stops moving. The fluid will then re-distribute into distinct pores. We don't know the microstructures this process would produce, but features as shown in Fig. 3f could indicate a healing grain boundary.

Conclusions

Single crystals of natural quartz containing fluid inclusions with different compositions have been deformed at temperatures ranging from 710-820°C, 1200 MPa confining pressure and 10^{-5}-10^{-6} strain rate, followed by an annealing stage under stress at temperatures between 800-900°C for 1-280 hours. Samples with gaseous fluid inclusions have a significantly higher strength than samples with aqueous inclusions. After the experiments the samples contain between 1 and 30% recrystallized grains. These grains are elongated perpendicular to the shortening direction. The recrystallized grains contain fewer fluid inclusions then the starting material, but have more fluid inclusions on their grain boundaries, indicating that the fluid is swept along by the boundary during migration.

Acknowledgements

We are indebted to Ben Kreulen, Prof. Touret and Steve Cox for supplying sample material from Naxos, Scandinavia and Victoria respectively, and Steve Cox for help with collecting quartz samples. This work was sponsored by a NWO Huygens fellowship to JLU. Harry Green and the late Tracy Tingle are thanked for introducing JLU to using the Griggs rig. G. Kastelijn and E. de Graaf are gratefully acknowledged for technical assistance. ADP likes to thank P. Fokker for useful and stimulating discussions and for supplying a workspace. We are grateful to J. Severstone and H. Stünitz for thorough and constructive reviews. In particular we would like to acknowldge John Fitz Gerald for his review and editorial help.

References

Aines R.D. & G.R. Rossman (1984) Water in minerals? A peak in the infrared. Journal of Geophysical Research 89: 4059-4072. 10.1029/JB089iB06p04059

Atkinson A. (1984) Diffusion along grain boundaries and dislocations in oxides, alkali halides and carbides. Solid State Ionics 12: 309-320. 10.1016/0167-2738(84)90160-7

Audétat, A. & D. Günther (1999) Mobility and H2O loss from fluid inclusions in natural quartz crystals. Contributions to Mineralogy and Petrology 137: 1-14. 10.1007/s004100050578

Bai, Q., Jin Z.-M. & H.W. Green II (1997) Experimental investigation of the rheology of partially molten peridotite at upper mantle pressures and temperatures. In: Deformation-enhanced fluid transport in the Earth's Crust and Mantle, ed. M.B. Holness. The Mineralogical Series 8: 40-61.

Bakker, R.J. & J.B.H. Jansen. (1991) Experimental post-entrapment water loss from synthetic CO2-H2O inclusions in natural quartz. Geochimica Cosmochimica Acta 55: 2215-2230. 10.1016/0016-7037(91)90098-P

Bakker, R.J. & J.B.H. Jansen (1994) A mechanism for preferential H2O leakage from fluid inclusions in quartz based on TEM observations. Journal of Geophysical Research 79: 1647-1652.

den Brok, B. (1992) An experimental investigation into the effect of water on the flow of quartzite. PhD thesis Univ. Utrecht. Geologica Ultraiectina 95: 178pp.

Bodnar, D.L., P.R. Binns, & D.L. Hall. (1989) Synthetic fluid inclusions - VI. Quantitative evaluation of the decrepitation behaviour of fluid inclusions in quartz at one atmosphere confining pressure. Journal of Metamorphic Geology 7: 229-242. 10.1111/j.1525-1314.1989.tb00586.x

Chernak L.J., G. Hirth, J. Selverstone, J. Tullis (2009) Effects of aqueous and carbonic fluids on the dislocation creep strength of quartz. Journal of Geophysical Research-Solid Earth, 114, 10.1029/2008JB005884

Dijkstra I. (1990) The Effects of Dynamic Recrystallization on Fluid Inclusions. Unpublished Master Thesis, Utrecht University, The Netherlands.

Dresen, G., Z. Wang, & Q. Bai, Q. (1996) Kinetics of grain growth in anorthite. Tectonophysics 258: 251-262 10.1016/0040-1951(95)00203-0

Drury, M.R. & J.L. Urai (1990) Deformation-related recrystallization. Tectonophysics 172: 235-253. 10.1016/0040-1951(90)90033-5

Drury, M.R. & J.D. Fitz Gerald (1996) Grain boundary melt films in an experimentally deformed olivine-orthopyroxene rock: implications for melt distribution in upper mantle rocks. Geophysical Research Letters 23: 701-704. 10.1029/96GL00702

Fisher, J.R. (1976) The volumetric properties of H2O - a graphical portrayal. Journal of Research of the U.S. Geological Survey, 4: 189-193.

Fitz Gerald, J.D., J.N. Boland, A.C. McLaren, A. Ord, & B.E. Hobbs (1991) Microstructures in water-weakened single crystals of quartz. Journal of Geophysical Research 96: 2139-2155. 10.1029/90JB02190

Hall, D.L. & S.M. Sterner (1993) Preferential water loss from synthetic fluid inclusions. Contributions to Mineralogy and Petrology 114: 489-500. 10.1007/BF00321753

Herwegh, M. & A. Berger. (2004) Deformation mechanisms in Zener dragged systems and their microstructural energy balance. Journal of Structural Geology 26: 1483–1498. 10.1016/j.jsg.2003.10.006

Hippert, J. & M. Egydio-Silva (1996) New polygonal grains formed by dissolution– redeposition in quartz mylonite. Journal of Structural Geology 18: 1345–1352.

Hirth, G. & Tullis (1992) Dislocation creep regimes in quartz aggregates. Journal of Structural Geology 14: 145-159. 10.1016/0191-8141(92)90053-Y

Hollister, L.S. (1990) Enrichment of CO2 in fluid inclusions in quartz by removal of H2O during crystal-plastic deformation. Journal of Structural Geology 12: 895-901. 10.1016/0191-8141(90)90062-4

Holness, M. B. (1992) Equilibrium dihedral angles in the system quartz-CO2-H2O-NaCl at 800ºC and 1–15 kbar: The effects of pressure and fluid composition on the permeability of quartzites: Earth and Planetary Science Letters 114: 171–184. 10.1016/0012-821X(92)90159-S

Holness, M.B. (1993) Temperature and pressure dependence of quartz-aqueous fluid dihedral angles: the control of adsorbed H2O on the permeability of quartzites. Earth and Planetary Science Letters 117: 363-377. 10.1016/0012-821X(93)90090-V

Holness, M.B. (1995) The effect of feldspar on quartz-H2O-CO2 dihedral angles at 4 kbar, with consequences for the behaviour of aqueous fluids in migmatites. Contributions to Mineralogy and Petrology 118: 356-364. 10.1007/s004100050020

Jaoul O., J Tullis & A.K Kronenberg (1984) The effect of varying water contents on the creep behavior of Heavitree quartzite. Journal of Geophysical Research 89: 4298–4312. 10.1029/JB089iB06p04298

Jin, Z.-M., H.W. Green, & Y. Zhou (1994) Melt topology in partially molten mantle peridotite during ductile deformation. Nature 372: 164-167. 10.1038/372164a0

Johannes, W. (1978) Pressure comparing experiments with NaCl, AgCl, talc and pyrophyllite assemblies in a piston cylinder apparatus. Neues Jahrbuch für Mineralogie 3: 84-92.

Johnson, E.L. & L.S. Hollister (1995) Syndeformational fluid trapping in quartz - determining the pressure-temperature conditions of deformation from fluid inclusions and the formation of pure CO2 fluid inclusions during grain boundary migration. Journal of Metamorphic Geology 13: 239-249. 10.1111/j.1525-1314.1995.tb00216.x

Karato, S.,-I. & T. Masuda (1989) Anisotropic grain growth in quartz aggregates under stress and its implication for foliation development. Geology 17: 695-698. 10.1130/0091-7613(1989)017<0695:AGGIQA>2.3.CO;2

Kekulawala, K.R.S.S., Paterson, M.S., Boland, J.N. (1978) Hydrolytic weakening in quartz. Tectonophysics 46: T1-T6. 10.1016/0040-1951(78)90101-4

Keppler H., Rauch, M. (2000) Water solubility in nominally anhydrous minerals measured by FTIR and H NMR. Physics and Chemistry of Minerals 27: 371 - 376. 10.1007/s002699900070

Kerrich, R. (1976) Some effects of tectonic recrystallization on fluid inclusions in vein quartz. Contributions to Mineralogy and Petrology 59: 195-202. 10.1007/BF00371308

Kronenberg, A.K., P. Segall & G.H. Wolf (1990) Hydrolytic weakening and penetrative deformation within a natural shear zone. In: The Brittle-Ductile Transition in Rocks (The Heard Volume), A. G. Duba, W. B. Durham, J. W. Handin, and H. F. Wang, Eds. Geophysical Monograph of the American Geophysical Union 56: 21-36.

Laporte, D. (1994) Wetting behavior of partial melts during crustal anatexis: the distribution of hydrous silicic melts in polycrystalline aggregates of quartz. Contributions to Mineralogy and Petrology 116: 486-499. 10.1007/BF00310914

Mancktelow, N.S., D. Grujic, & E.L. Johnson (1998) An SEM study of porosity and grain boundary microstructure in quartz mylonites, Simplon Fault Zone, Central Alps. Contributions to Mineralogy and Petrology 131: 71-85. 10.1007/s004100050379

Mavrogenes, J.A. & R.J. Bodnar (1994) Hydrogen movement into and out of fluid inclusions in quartz: experimental evidence and geologic implications. Geochimica Cosmochimica Acta 58: 141-148. 10.1016/0016-7037(94)90452-9

McLaren, A.C., J.D. Fitz Gerald, & J. Gerretsen (1989) Dislocation nucleation and multiplication in synthetic quartz: relevance to water weakening. Physics and Chemistry of Minerals 16: 465–482. 10.1007/BF00197016

Morgan, G.B., I-M. Chou, J.D. Pasteris, & S.N. Olsen (1993) Re-equilibration of CO2 fluid inclusions at controlled hydrogen fugacities. Journal of Metamorphic Geology 11: 155-164. 10.1111/j.1525-1314.1993.tb00137.x

Olgaard, D.L. & B. Evans (1988) Grain growth in synthetic marbles with added mica and water. Contributions to Mineralogy and Petrology 100: 246-260. 10.1007/BF00373591

Olgaard, D.L. & J.D. Fitz Gerald (1993) Evolution of pore microstructures during healing of grain boundaries in synthetic calcite rocks. Contributions to Mineralogy and Petrology 215: 138-154. 10.1007/BF00321216

Ord, A. & B.E. Hobbs (1986) Experimental control of the water-weakening effect in Quartz. In: Mineral and Rock Deformation; Laboratory Studies - The Paterson Volume, B.E. Hobbs and H.C. Heard, Eds., Geophysical Monograph of the American Geophysical Union 36: 51-65.

Paterson, M.S. (1986) The thermodynamics of water in quartz. Phys. Chem. Minerals, 13: 245-55. 10.1007/BF00308276

Paterson, M.S. (1989) The interaction of water with quartz and its influence in dislocation flow - an overview. In: S.-I. Karato and M. Toriumi (Editors), Rheology of Solids and of the Earth, Oxford University Press, Oxford: 107-142.

Post, A.D. & J. Tullis (1998) The rate of water penetration in experimentally deformed quartzite: implications for hydrolytic weakening. Tectonophysics 295: 117–138. 10.1016/S0040-1951(98)00145-0

Post, A.D., J.Tullis & R.A. Yund (1996) Effect of chemical environment on dislocation creep of quartzite. J. Geoph.Res. 101: 22143-22155 10.1029/96JB01926

Roedder, E. (1984) Fluid inclusions. Reviews in Mineralogy 12. Mineralogical Society of America: 644 pp.

Rutter, E. H. & K.H. Brodie (2004) Experimental intracrystalline plastic flow in hot-pressed synthetic quartzite prepared from Brazilian quartz crystals. Journal of Structural Geology 26: 259-270. 10.1016/S0191-8141(03)00096-8

Schenk, O. & J.L. Urai (2005) The migration of fluid-filled grain boundaries in recrystallizing synthetic bischofite: first results of in-situ high-pressure, high temperature deformation experiments in transmitted light. Journal of Metamorphic Geology 23 (8): 695-709. 10.1111/j.1525-1314.2005.00604.x

Schmatz, J., O. Schenk & J.L. Urai. (2011) The effect of fluid inclusion-grain boundary interaction on grain boundary migration recrystallization - results from annealing experiments on different rock analogue-pore fluid systems. Contributions to Mineralogy and Petrology 162: 193–208. 10.1007/s00410-010-0590-3

Schmatz, J. & J.L. Urai (2010). The interaction of fluid inclusions and migrating grain boundaries in a rock analogue: deformation and annealing of polycrystalline camphor-ethanol mixtures. Journal of Metamorphic Geology 28: 1-18. 10.1111/j.1525-1314.2009.00849.x

Schmatz, J. & J.L. Urai (2011) The interaction of migrating grain boundaries and fluid Inclusions in naturally deformed quartz: a case study of a folded and partly recrystallized quartz vein from the Hunsrück Slate, Germany. Journal of Structural Geology 33: 468-480. 10.1016/j.jsg.2010.12.010

Schuiling, R.D & R. Kreulen. (1979) Are thermal domes heated by CO2-rich fluids from the mantle? Earth and Planetary Science Letters 43: 298-302. 10.1016/0012-821X(79)90214-0

Selverstone J. (2005) Preferential embrittlement of graphitic schists during extensional unroofing in the Alps: the effect of fluid composition on rheology in low-permeability rocks. Journal of Metamorphic Geology 23: 461–470. 10.1111/j. 1525-1314.2005.00583.x

Sterner, S.M. & R.J. Bodnar (1989) Synthetic fluid inclusions. VII. Re-equilibration of fluid inclusions in quartz during laboratory-simulated metamorphic burial and uplift. Journal of Metamorphic Geology 7: 243-260. 10.1111/j. 1525-1314.1989.tb00587.x

Stipp, M., J. Tullis, & H. Behrens (2006) Effect of water on the dislocation creep microstructure and flow stress of quartz and implications for the recrystallized grain size piezometer. Journal of Geophysical Research 111: B04201. 10.1029/2005JB003852

Tarantola, A., L.E. Diamond, & H. Stünitz (2011) Modification of fluid inclusions in quartz by deviatoric stress I: experimentally induced changes in inclusion shapes and microstructures. Contributions to Mineralogy and Petrology 160: 825-843. 10.1007/s00410-010-0509-z

Tullis J. & R. Yund (1982) Grain growth kinetics of quartz and calcite aggregates. Journal of Geology 90: 661-665. 10.1086/628681

Tullis, T.E. & J. Tullis (1986) Experimental rock deformation techniques. In: Mineral and Rock Deformation; Laboratory Studies - The Paterson Volume, B.E. Hobbs and H.C. Heard, Eds., Geophysical Monograph of the American Geophysical Union 36: 297-324.

Tullis, J., R. Yund, & J. Farver (1996) Deformation-enhanced fluid distribution in feldspar aggregates and implications for ductile shear zones. Geology 24: 63-66. 10.1130/0091-7613(1996)024<0063:DEFDIF>2.3.CO;2

Urai J.L. (1983) Deformation of wet salt rocks: an investigation into the interaction between mechanical properties and microstructural development during deformation of polycrystalline carnallite and bischofite in the presence of a pore fluid. PhD Thesis, Univ. Utrecht, 221pp.

Urai J.L., W.D. Means, & G.S. Lister (1986) Dynamic recrystallization of minerals. In: Mineral and Rock Deformation; Laboratory Studies - The Paterson Volume, B.E. Hobbs and H.C. Heard, Eds., Geophysical Monograph of the American Geophysical Union 36: 161-199.

Urai J.L., C.J. Spiers, H.J. Zwart, & G.S. Lister (1986) Weakening of rock salt by water during long-term creep. Nature 324: 554-557. 10.1038/324554a0

Vityk, M.O., R.J. Bodnar, & J.C. Doukhan. (2000) Synthetic fluid inclusions: XV. TEM investigation of plastic flow associated with reequilibration of fluid inclusions in natural quartz: Contributions to Mineralogy and Petrology 139: 285–297. 10.1007/s004100000142

Wang, J.N., J.N. Boland, A. Ord, & B.E. Hobbs (1993) Microstructural and defect development in heat treated heavitree quartzite. defects and processes in the solid state: geoscience applications. The McLaren volume. eds. J.N. Boland and J.D. FitzGerald: 359-381.

Wang, J.N. (1992) Creep of quartz polycrystal in controlled chemical environments. PhD thesis Monash Univ. Australia: 239pp.

Watson, E.B., J.M. Brenan, & D.R. Baker (1990) Distribution of fluids in the continental mantle. In: Continental Mantle (ed. Menzies, M.A.). Oxford Monographs on Geology and Geophysics 16: 111-125.